J|A|C|S

A R T I C L E S

Molecular Recognition and Fluorescence Sensing of Monophosphorylated Peptides in Aqueous Solution by Bis(zinc(II)−dipicolylamine)-Based Artificial Receptors

Akio Ojida,[†] Yasuko Mito-oka,[†] Kazuki Sada,[†] and Itaru Hamachi*,[†,‡,§]

Contribution from the PRESTO (Organization and Function, JST), Institute for Materials Chemistry and Engineering (IMCE), Department of Chemistry and Biochemistry, Graduate School of Engineering, and Kyushu University, Fukuoka, 812-8581, Japan

Received September 2, 2003; E-mail: itarutcm@mbox.nc.kyushu-u.ac.jp

Abstract: The phosphorylation of proteins represents a ubiquitous mechanism for the cellular signal control of many different processes, and thus selective recognition and sensing of phosphorylated peptides and proteins in aqueous solution should be regarded as important targets in the research field of molecular recognition. We now describe the design of fluorescent chemosensors bearing two zinc ions coordinated to distinct dipicolylamine (Dpa) sites. Fluorescence titration experiments show the selective and strong binding toward phosphate derivatives in aqueous solution. On the basis of ^{1}H NMR and ^{31}P NMR studies, and the single-crystal X-ray structural analysis, it is clear that two Zn(Dpa) units of the binuclear receptors cooperatively act to bind a phosphate site of these derivatives. Good agreement of the binding affinity estimated by isothermal titration calorimetry with fluorescence titration measurements revealed that these two receptors can fluorometrically sense several phosphorylated peptides that have consensus sequences modified with natural kinases. These chemosensors display the following significant features: (i) clear distinction between phosphorylated and nonphosphorylated peptides, (ii) sequence-dependent recognition, and (iii) strong binding to a negatively charged phosphorylated peptide, all of which can be mainly ascribed to coordination chemistry and electrostatic interactions between the receptors and the corresponding peptides. Detailed titration experiments clarified that the phosphate anion-assisted coordination of the second Zn(II) to the binuclear receptors is crucial for the fluorescence intensification upon binding to the phosphorylated derivatives. In addition, it is demonstrated that the binuclear receptors can be useful for the convenient fluorescent detection of a natural phosphatase (PTP1B) catalyzed dephosphorylation.

Introduction

The phosphorylation of proteins, triggered in response to extracellular signals, represents a ubiquitous mechanism for the cellular control of many different processes, including metabolic pathways, cell growth and differentiation, membrane transport, and apoptosis.[1] In signal transduction cascades, phosphorylation on serine, threonine, and tyrosine residues on protein surfaces induces a specific protein−protein interaction, often including the phosphoprotein binding domain such as the SH2, WW, and FHA domains.[2] Protein phosphorylation also allosterically regulates the catalytic activity of an enzyme through induction of conformational changes.[3] On the other hand, the reverse reaction of dephosphorylation is catalyzed by protein phosphatase. It is known that signal transduction is controlled by the balance of phosphorylation/dephosphorylation in time-specific and spatiospecific ways in a living cell.

To elucidate such complicated signal transduction events, it is desirable to develop versatile methods and molecular probes which can selectively recognize phosphorylated proteins using convenient techniques. Several groups have devoted much effort toward the development of molecular devices that can fluorometrically sense protein phosphorylation events, however, most of which are based on natural peptides or protein scaffolds to detect the activation of certain protein kinases through their own phosphorylations.[4] We are interested in the development of small molecules that can directly interact with a phosphate group on protein surfaces. These artificial receptors may allow one to sense and regulate the phopshorylation/dephosphrylation events.

We have briefly reported a new class of artificial receptors, the anthracene bis(zinc(II)−dipicolylamine) complexes, which
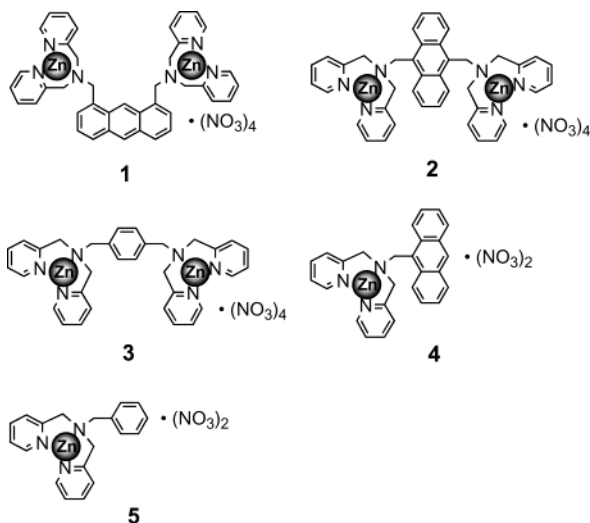
† PRESTO.
‡ IMCE, Department of Chemistry and Biochemistry.
§ Graduate School of Engineering.
(1) Sefton, B. M.; Hunter, T. *Protein Phosphorylation*; Academic Press: New York 1998.
(2) (a) Pawson, T.; Raina, M.; Nash, P. *FEBS Lett.* **2002**, *513*, 2. (b) Pawson, T.; Gish, G. D.; Nash, P. *Trends Cell Biol.* **2001**, *11*, 504. (c) Macias, M. J.; Wiesner, S.; Sudol, M. *FEBS Lett.* **2002**, *513*, 30. (d) Durocher, D.; Jackson, S. P. *FEBS Lett.* **2002**, *513*, 58. (e) Yaffe, M. B.; Elia, A. EH. *Curr. Opin. Cell Biol.* **2001**, *13*, 131.
(3) Johnson, L. N.; Lewis, R. J. *Chem. Rev.* **2001**, *101*, 2209.

(4) (a) Yeh, R.-H.; Yan, X.; Cammer, M.; Bresnick, A. R.; Lawrence, D. S. *J. Biol. Chem.* **2002**, *277*, 11527. (b) Chen, C.-A.; Yeh, R.-H.; Lawrence, D. S. *J. Am. Chem. Soc.* **2002**, *124*, 3840. (c) Sato, M.; Ozawa, T.; Inukai, K.; Asano, T.; Umezawa, Y. *Nat. Biotechnol.* **2002**, *20*, 287. (d) Kurokawa, K.; Mochizuki, N.; Ohba, Y.; Mizuno, H.; Miyawaki, A.; Matsuda, M. *J. Biol. Chem.* **2001**, *276*, 31305. (e) Nagai, Y.; Miyazaki, M.; Aoki, R.; Zama, T.; Inouya, S.; Hirose, K.; Iino, M.; Hagiwara, M. *Nat. Biotechnol.* **2000**, *18*, 313. (f) Ng, T.; Squire, A.; Hansra, G.; Bornancin, F.; Prevostel, C.; Hanby, A.; Harris, W.; Barnes, D.; Schmidt, S.; Mellor, H.; Bastiaens, P. I. H.; Parker, P. J. *Science* **1999**, *283*, 2085.

Chart 1. Molecular Structure of the Artificial Receptors and the Derivatives Discussed Here

Figure 1. Fluorescence spectral change of **1** (5 μM) upon the addition of *O*-phospho-L-tyrosine (p-Tyr): [p-Tyr] = 2.5, 5, 7.5, 10 15, 20, and 25 μM in 10 mM HEPES buffer, pH 7.2 at 20 °C, λ_{ex} = 370 nm. (inset) Job plot fluorescently examined between receptor **1** and p-Tyr (total concentration is 10 μM).

can bind and fluorescently sense phosphorylated peptides.[5] In the present paper, we describe the details of the binding properties of the receptors with phosphate species by NMR and X-ray crystallographic studies and sequence-dependent binding toward phosphorylated peptides by fluorescence and ITC experiments. We also discuss herein the fluorescence sensing mechanism of the receptors toward phosphorylated peptides. The obtained data indicate that the fluorescence intensification upon binding to phosphate species is mainly due to phosphate anion-induced Zn(II) complexation to the second dipicolylamine (Dpa) site of the receptors. Furthermore, we employ the present receptors for monitoring an enzymatic dephosphorylation process, in which the phosphatase-catalyzed dephosphorylation of a substrate peptide can be fluorometrically traced.

Results and Discussion

Molecular Design. We initially designed artificial molecules that can interact with phosphate species in aqueous solution. The structures of the artificial receptors **1** and **2** are depicted in Chart 1. Although a number of phosphate-specific artificial receptors and chemosensors have been reported,[6] only a few of them that efficiently work under aqueous conditions have been developed.[7] This is partially attributed to the general difficulty in the designing of artificial molecules that can efficiently bind to anions in aqueous solution by means of hydrogen bonding or electrostatic interaction. We planned to utilize a metal–ligand interaction (i.e., coordination chemistry) as the main force to bind phosphate species, since this interaction works in water more effectively than other interactions such as hydrogen bonding and ion-pair interaction. Binuclear metallophosphatase, such as alkaline phosphatase that catalyzes the hydrolysis
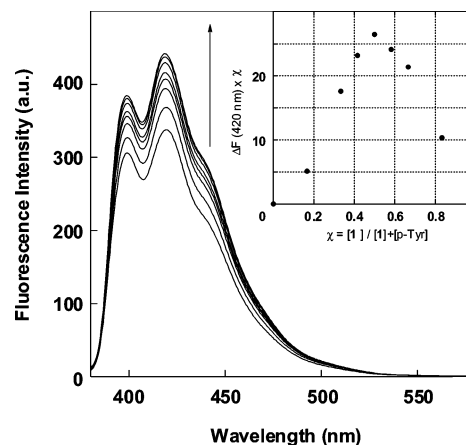
reaction of the phosphate ester, possesses two Zn(II) ions in close proximity in its active site.[8] The X-ray crystal structure of alkaline phosphatase complexed with an alkyl phosphate revealed that the phosphate site is bidentately bound to the two zinc ions. This structure gave us an important clue in designing the artificial receptor. In the designed receptors, the two sets of Zn(II)–Dpa are juxtaposed separately at an appropriate distance and are used as the binding motif toward phosphate species. An anthracene ring connecting two Dpas is employed not only as a spacer but also as a fluorophore, in which it may be expected that the binding event can be detected by a fluorescence signal.

The artificial receptors **1** and **2** were synthesized from the corresponding bis-halomethylanthracene by treatment with 2,2′-dipicolylamine followed by complexation with 2 equiv of zinc(II) nitrate. Using the same procedures, we also prepared the receptor **3** as a structurally related analogue of **2** and receptors **4** and **5** as monodentate control compounds. Characterization of these compounds was accomplished using ^{1}H NMR, mass spectrometry, and elemental analysis.

Anion Selectivity in Fluorescent Sensing. Under aqueous neutral conditions (10 mM HEPES, pH 7.2), the binuclear receptor **1** displays a fluorescence at 420 nm due to the anthracene, and the fluorescence intensity increases upon the addition of phosphorylated species such as phosphate anion, and phosphate monoesters (phenyl phosphate (PhP), *o*-phospho-l-tyrosine (p-Tyr), and methyl phosphate (MeP)) as shown in Figure 1. The titration experiments obey a typical saturation curve depending on the concentration of the phosphate derivatives (see Supporting Information). In the Job plot, the maximum fluorescence change was observed when the molar ratio of receptor **1** and p-Tyr was equivalent, indicative of a 1:1 complex (inset of Figure 1). Similar fluorescence changes and a 1:1 binding stoichiometry were also observed in the case of receptor **2**.[5] Table 1 summarizes the apparent binding constants (K_{app}, M^{-1}) thus estimated. These receptors showed a high affinity toward the monophosphate derivatives with 10^5–10^4 M^{-1} of the binding constants.[9] In contrast, no fluorescence change was induced by other anions such as carbonate, sulfonate, nitrate,

(5) Ojida, A.; Mito-oka, Y.; Inoue, M.; Hamachi, I. *J. Am. Chem. Soc.* **2002**, *124*, 6256.

(6) Beer, P. D.; Gale, P. A. *Angew. Chem., Int. Ed.* **2001**, *40*, 486.

(7) Artificial receptor and chemosensor for phosphate species that work in aqueous solution: (a) Aoki, S.; Kimura, E. *Rev. Mol. Biotechnol.* **2002**, *90*, 129. (b) Lee, D. H.; Im, J. H.; Son, S. U.; Chung, Y. K.; Hong, J.-I. *J. Am. Chem. Soc.* **2003**, *125*, 7752. (c) Tobey, S. L.; Jones, B. D.; Anslyn, E. V. *J. Am. Chem. Soc.* **2003**, *125*, 4026. (d) Han, M. S.; Kim, D. H. *Angew. Chem., Int. Ed.* **2002**, *41*, 3809. (e) Mizukami, S.; Nagano, T.; Urano, Y.; Odani, A.; Kikuchi, K. *J. Am. Chem. Soc.* **2002**, *124*, 3920. (f) Vance, D. H.; Czarnik, A. W. *J. Am. Chem. Soc.* **1994**, *116*, 9397. (g) Hosseini, M. W.; Blacker, A. J.; Lehn, J.-M. *J. Am. Chem. Soc.* **1990**, *112*, 3896.

(8) (a) Lipscomb, W. N.; Sträter, N. *Chem. Rev.* **1996**, *96*, 2375. (b) Wilcox, D. E. *Chem. Rev.* **1996**, *96*, 2435.
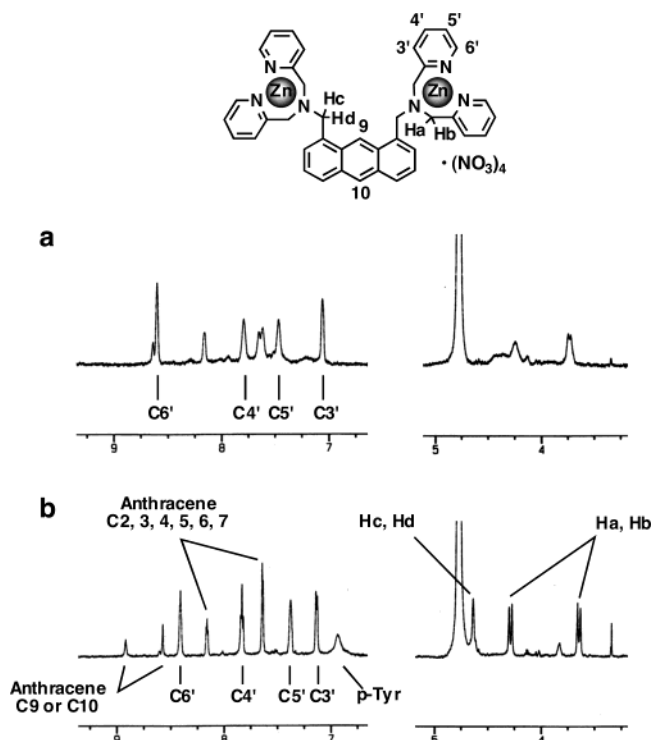
Table 1. Summary of the Apparent Binding Constant (K_{app}, M^{-1}) of Receptors **1** and **2** to the Phosphate Species by Fluorescence Change

phosphate species[a]	receptor		phosphate species[a]	receptor	
	1	2		1	2
NaH_2PO_4[b]	4.2×10^5	2.9×10^5	ATP[c]	$>10^7$	4.0×10^5
PhP[b]	2.1×10^5	5.1×10^4	ADP[c]	$>10^7$	1.6×10^5
p-Tyr[b]	3.1×10^5	6.1×10^5	AMP[c]	2.3×10^5	9.1×10^3
MeP[b]	1.1×10^5	7.9×10^3	cAMP[c]	d	d
diMeP[b]	d	d			

[a] PhP= phenyl phosphate, p-Tyr = *O*-phospho-L-tyrosine, MeP = methyl phosphate, diMeP = dimethyl phosphate, ATP = adenosine 5′-triphosphate, ADP = adenosine 5′-diphosphate, AMP = adenosine 5′-monophosphate, cAMP = adenosine 3′,5′-cyclic monophosphate. [b] Measurement conditions: 10 mM HEPES, pH 7.2, 20 °C. [c] Measurement conditions: 50 mM HEPES, 50 mM NaCl, pH 7.2, 20 °C. [d] Since the fluorescence change was scarcely observed, the association constant cannot be obtained.

acetate, and chloride up to the millimolar concentration range.[5] These results revealed that receptors **1** and **2** are fluorescent chemosensors with a high selectivity toward phosphate derivatives among the various anions. The receptors showed the stronger binding affinity toward the pyrophosphate derivatives such as ATP and ADP compared to the monophosphate species. Interestingly, dimethyl phosphate (diMeP) and cyclic AMP (cAMP) did not cause any fluorescence change up to the millimolar concentration range (see Supporting Information), suggesting that receptors **1** and **2** can distinguish phosphate and phosphate monoesters from phosphate diesters. The mononuclear receptor **4**, on the other hand, did not show any significant fluorescence changes for these phosphate derivatives (data not shown). Therefore, the affinity of the mononuclear Zn(II)−Dpa complex toward phosphate derivatives was evaluated by a fluorescence competitive inhibition experiment using the mono Zn(II)−Dpa receptor **5** and the binuclear receptor **2**.[10] The apparent binding constant of **5** for phenyl phosphate was estimated to be $(3-4) \times 10^3$ M^{-1}, which is 1 or 2 orders of magnitude lower than those of **1** or **2**. These results suggest that the two Zn(II)−Dpa sites are indispensable for tight binding and sensing of phosphate derivatives in aqueous solution.

Binding Mode of the Zn(Dpa)-Based Receptors to Phosphate Species. A ^{1}H NMR study of **1** in D_2O (pD 7.1 ± 0.1) allowed us elucidation of the structure of **1** complexed with p-Tyr in aqueous solution. Figure 2 shows the ^{1}H NMR signals of the aromatic and methylene regions of **1**. Upon the addition of 1 equiv of p-Tyr to receptor **1**, the proton signals of the pyridine ring of two Dpas slightly upfield-shifted (0.09−0.18 ppm) and the corresponding proton signals were not distinguished among the four pyridine rings of the two sets of Dpas. Furthermore, two sets of three methylene protons connected to the tertiary nitrogen (4.63, 4.29, and 3.65 ppm) became sharper upon the p-Tyr binding. These observations suggest that the two Zn(II)−Dpa sites equally contribute to the binding to p-Tyr. In the ^{31}P NMR study, the chemical shift due to the phosphorus of p-Tyr moved from −2.09 to −3.00 ppm upon the addition of 1 equiv of **1** (see Supporting Information). The receptor-

(9) The binding affinities (K_{app}, M^{-1}) of receptor **1** to phenyl phosphate (PhP) in the presence of biologically abundant metal ions are determined by the fluorescence titration as follows: $K_{app} = 8.1 \times 10^4$ (10 mM $CaCl_2$), 5.8×10^4 (10 mM $MgCl_2$), 2.6×10^4 (100 mM NaCl), and 2.3×10^4 (100 mM KCl) M^{-1}. These results indicate that the presence of the metal ions slightly suppresses the binding affinity because of the increase of ionic strength, but the sort of metal cation did not affect the binding constant. Almost the same trend was observed in the case of receptor **2**.
(10) Diederich, F.; Dick, K. *J. Am. Chem. Soc.* **1984**, *106*, 8024.

Figure 2. ^{1}H NMR spectra of **1** (0.1 mM) in the absence (a) and presence (b) of 1 equiv of p-Tyr measured in D_2O, pD 7.1 ± 0.1.

induced upfield shift of the ^{31}P NMR signal was similarly observed in the case of phenyl phosphate (from −2.72 to −3.94 ppm) and a phosphorylated peptide KSGpYLSSE (from −2.12 to −2.90 ppm). These results indicate that receptor **1** directly interacts with the phosphate site in aqueous solution.

The binding mode of the receptors with phosphate derivatives was unequivocally determined by X-ray crystallographic analysis of a complex of **1** with phenyl phosphate (PhP). An equimolar mixture of **1** and PhP in MeOH−acetone gave a colorless prism suitable for an X-ray analysis. The X-ray analysis revealed that **1** and PhP form a dimer complex related by a symmetric center in the unit cell as shown in Figure 3a.[11,12] In the asymmetric half-unit (Figure 3b), PhP is incorporated between two zinc ions by coordination of phosphate oxygen atoms of PhP to the two metal sites in the same molecule. Both Zn(II) ions have the disordered tetragonal-pyramidal five-coordinated state, where the Zn(II) ions are coordinated by the three nitrogen atoms of the Dpa site and the phosphate oxygen atom of PhP. One of the two metal cations is bound to nitrate anion and the other is bound to the phosphate oxygen atom of

(11) Generally speaking, it is difficult to demonstrate that a crystal structure obtained by recrystallization is the same as a structure in aqueous solution, because of additional effects such as crystal packing and high concentration in crystal growth. In the present case, we do not have enough data to rule out the possibility of the 2:2 complex in aqueous solution. However, we consider that the 2:2 complex of **1** with phenyl phosphate can be only formed in the crystalline state because of the following reasons. (i) In the case of the peptide as a binding guest, the 2:2 complex is not plausible due to the steric hindrance and electrostatic repulsion between the corresponding peptides. (ii) According to ITC and fluorescence titration data, the binding mode of the receptor to the peptides is identical with that to phosphorylated small molecules such as p-Tyr and phenyl phosphate. (iii) We do not obtain any positive data to show the interaction between two anthracenes or two phenyl phosphates in a postulated 2:2 complex from ^{1}H NMR, ITC, and fluorescence titration conducted in aqueous medium.
(12) Such 1:3 coordination between an anionic phosphate with Zn(II) complexes has been also reported: Kimura, E.; Aoki, S.; Koike, T.; Shiro, M. *J. Am. Chem. Soc.* **1997**, *119*, 3068.
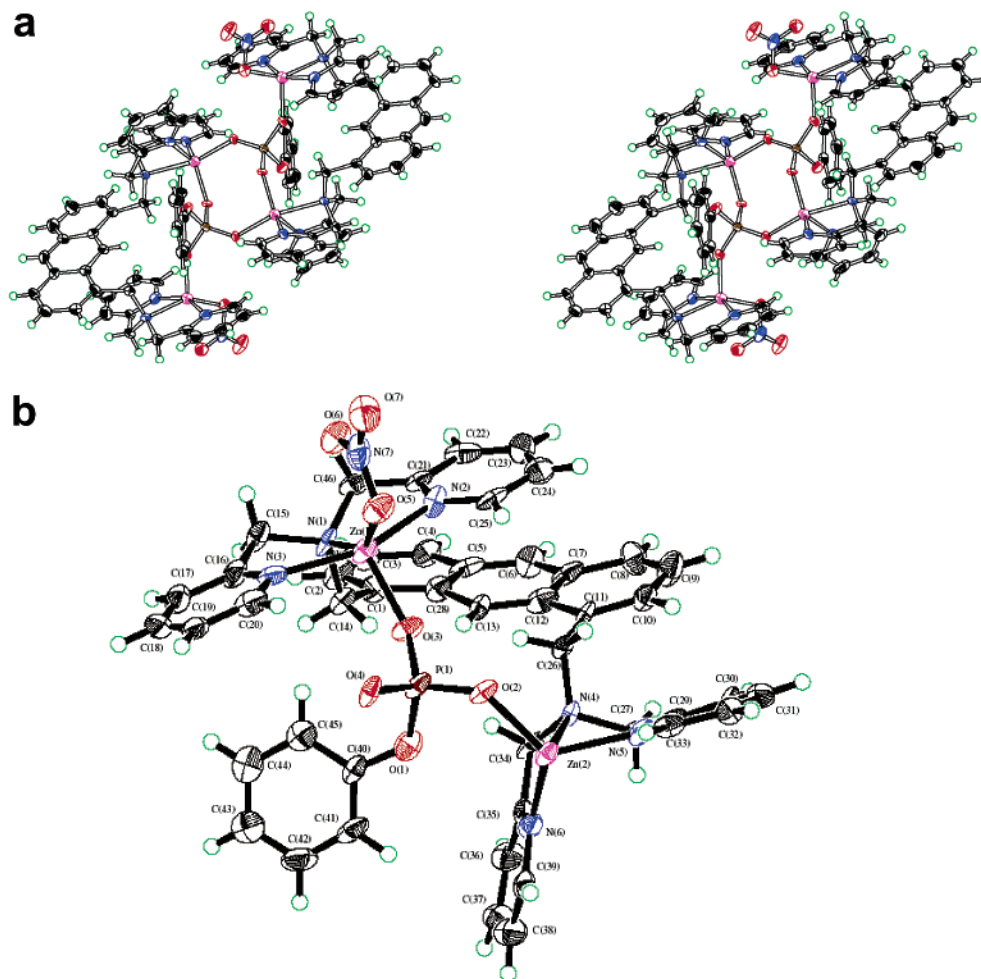
Figure 3. ORTEP drawing (50% probability ellipsoids) of the complex of **1** with phenyl phosphate: (a) stereoimage of a dimer complex; (b) an asymmetrical half unit of the complex. Disordered nitrate anions are omitted for clarity.

Table 2. Amino Acid Sequences of the Peptides Containing the Optimal Consensus Sequences Phosphorylated by Different Protein Kinases and the Apparent Binding Constant (K_{app}, M^{-1}) of the Receptor **1** and **2** to the Peptides Determined by Fluorescence Change

	consensus substrate sequence	kinase	net charge	1	2
peptide-a:	Glu-Glu-Glu-Ile-**p**Tyr-Glu-Glu-Phe-Asp	v-Src	−8	8.9×10^6	9.5×10^5
peptide-b:	Asp-Glu-Glu-Ile-**p**Tyr-Gly-Glu-Phe-Phe	c-Src	−6	1.5×10^6	3.6×10^5
peptide-c:	Arg-Arg-Phe-Gly-**p**Ser-Ile-Arg-Arg-Phe	Lck 1	−4	8.2×10^5	1.5×10^5
peptide-d:[a]	Lys-Ser-Gly-**p**Tyr-Leu-Ser-Ser-Glu	EGFR	−2	5.8×10^4	1.2×10^4
peptide-e:	Ala-Glu-Glu-Ile-**p**Tyr-Gly-Val-Leu-Phe	PKA	0	b	b
peptide-f:	Ala-Arg-Arg-Gly-**p**Ser-Ile-Ala-Ala-Phe	Bck1	+2	b	b
peptide-g:	Glu-Glu-Glu-Ile-Tyr-Glu-Glu-Phe-Asp	v-Src		b	b

[a] Amino acid sequence of ezrin (142−149) phosphorylated by EGFR. [b] Since the fluorescence change was scarcely observed, the binding constant cannot be obtained.

the neighboring PhP. The latter bridging coordination provides the dimeric complex as shown in Figure 3a. As a result, receptor **1** binds PhP by using the two sets of Zn(II)−Dpas through coordination. This cooperative action of the two Zn(II)−Dpa sites is quite consistent with the other experimental data in aqueous solution and reasonably explains the high affinity of **1** toward phosphate species compared to the monodentate receptors **4** and **5**.

Binding Selectivity and Fluorescence Sensing toward Phosphorylated Peptide. Subsequently, we tested the sensing capability of these receptors for several phosphorylated peptides. In a previous communication,[5] we preliminarily reported that the receptors could preferentially sense a sequence of a phosphorylated peptide with a rich negative charge, relative to

a positively charged one. To understand such a sequence-dependent recognition of these receptors in detail, we prepared six types of phosphorylated peptide sequences (peptide-a to peptide-f; see Table 2) and evaluated the binding affinity by fluorescence titration experiments. These peptides, possessing a distinct number of net charges from −8 to +2 (from peptide-a to peptide-f), contain the optimal consensus sequences phosphorylated by distinct protein kinases[13] with the exception of peptide-d which is the fragment of ezrin (142−149) phosphorylated by EGFR (epidermal growth factor receptor).[14] Figure 4a shows a typical fluorescence spectral change of **1** during

(13) (a) Songyang, Z.; Cantley, L. C. *Trends Biochem. Sci.* **1995**, 470. (b) Pinna, L. A.; Ruzzene, M. *Biochim. Biophys. Acta* **1996**, *1314*, 191.
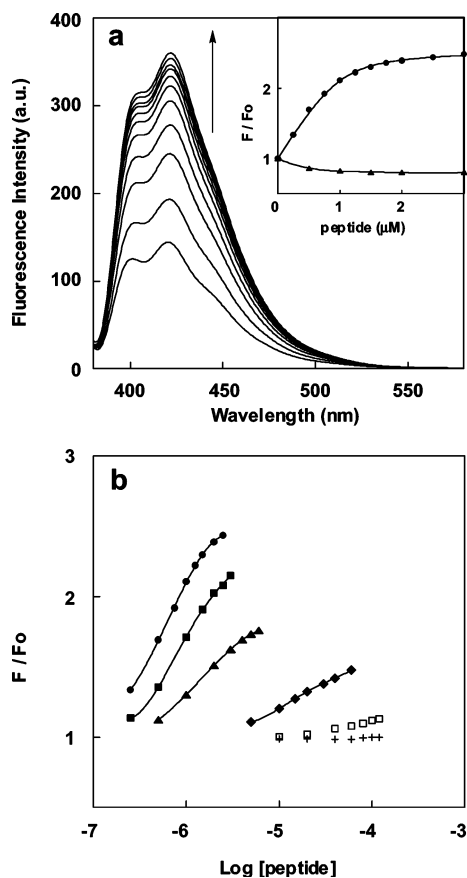(14) Krieg, J.; Hunter, T. *J. Biol. Chem.* **1992**, *267*, 19258.

Figure 4. (a) Fluorescence spectral change of **1** (1 μM) upon the addition of peptide-a: [peptide-a] = 0, 0.25, 0.5, 0.75, 1, 1.25, 1.5, 1.75, 2, 2.5, and 3 μM in 50 mM HEPES buffer, pH 7.2, 50 mM NaCl at 20 °C, and λ_{ex} = 370 nm. (Inset) Fluorescence titration curve of **1** (λ_{em} = 420 nm) with peptide-a (●) and peptide-g (▲). (b) Fluorescence titration profiles of **1** (λ_{em} = 420 nm) with the various phosphorylated peptides: peptide-a (●), peptide-b (■), peptide-c (▲), peptide-d (◆), peptide-e (□), and peptide-f (+).

titration with a phosphorylated peptide. The fluorescence intensity of **1** significantly increased (2.5-fold magnitude) by the addition of less than 2 μM of peptide-a, a consensus sequence phosphorylated by a protein kinase, v-Src. In sharp contrast, the fluorescence change scarcely took place by the corresponding nonphosphorylated peptide-g (inset of Figure 4a), showing that the receptors can clearly distinguish the phosphorylated peptides from a nonphosphorylated one. The saturation curve gave us the apparent binding constants (K_{app}, M^{-1}) for each peptide and these results are summarized in Figure 4b and Table 2. It is clear that the binding affinity strongly depends on the net charge of the phosphorylated peptide. Both receptors (**1** and **2**) can have the tightest binding with peptide-a having the largest negative charge (−8) with K_{app} of 10^7−10^6 M^{-1}. The binding constant of the receptors becomes greater with increase in the negative charge of the phosphorylated peptides. In the case of peptides-e and -f bearing the net charges of 0 and +2, respectively, the receptors can scarcely sense them even for 10^{-4} M of concentration. These data clearly indicate that the binding selectivity of the present receptors can be ascribed to the net charge of the phosphorylated peptides, as well as the coordination of Zn(II) to the phosphate unit. Interestingly, the magnitude of the fluorescence enhancement (F_{max}/F_o) also depends on the net charge of the peptide. In fact, peptide-a increased the fluorescence intensity most efficiently
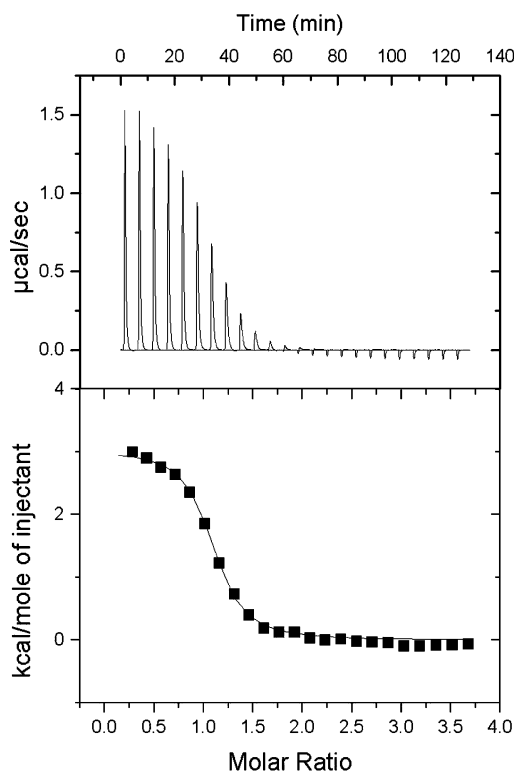

Figure 5. Typical ITC titration curve and processed data (for the titration of **1** with peptide-d), under the following conditions: [**1**] = 100 μM, [peptide-d] = 2.0 mM (24 × 10 μL injections), 50 mM HEPES buffer, pH 7.2, 25 °C.

(F_{max}/F_o = 2.5), and the value became smaller with the decreasing negative net charge of the peptides. This phenomenon is closely related to the mechanism of fluorescence change and is discussed later (vide infra).

Isothermal Titration Calorimetry Study of Phosphorylated Peptide Recognition. To discuss the binding features of the receptors toward a series of phosphorylated peptides in more detail, we next evaluated their interactions by isothermal titration calorimetry (ITC).[15] This technique provides the binding constant and stoichiometry as well as the thermodynamic parameters. A typical titration curve is shown in Figure 5. It is clear that the interaction of the receptor **1** with peptide-d is endothermic, indicating that the binding process is entropy-driven. Several examples in which entropy-driven endothermic interactions take place between anions and charged receptors have been reported.[16] In such cases, the release of solvent molecules from the solvation spheres of cations and anions results in the entropic overcompensation of the unfavorable positive ΔH of desolvation. The complex formation between metal cations and anionic species is a typical example.[17] The resultant data gave the stoichiometry (*n*), apparent binding constant (K_{app}), and the enthalpy (ΔH). The entropy values (ΔS) were calculated using the experimentally determined parameters (K_{app}, ΔH). Table 3 summarizes the results of the ITC experiments between the receptors and the phosphorylated peptides. Due to the aggregation property of receptor **2** under the high concentration necessary for the ITC measurement (25−

(15) Wadsö, I. *Chem. Soc. Rev.* **1997**, *26*, 79.
(16) (a) Rekharsky, M.; Inoue, Y.; Tobey, S.; Metzger, A.; Anslyn, E. *J. Am. Chem. Soc.* **2002**, *124*, 14959. (b) Kubik, S.; Kirchner, R.; Nolting, D.; Seidel, J. *J. Am. Chem. Soc.* **2002**, *124*, 12754.
(17) Herrero, L. A.; Terrón, A. *J. Biol. Inorg. Chem.* **2000**, *5*, 269.

Table 3. Stoichiometry (n), Binding Constant (K_{app}, M^{-1}), Enthalpy (ΔH, kcal mol^{-1}), and Entropy ($T\Delta S$, kcal mol^{-1}) for the Interactions of the Receptors with the Phosphorylated Peptides

receptor		peptide-a	peptide-b	peptide-c	peptide-d	peptide-e	peptide-f
1	n			0.88 ± 0.01	1.05 ± 0.01	0.93 ± 0.07	1.26 ± 0.48
	K_{app}	$>10^7$	b	$(1.81 \pm 0.38) \times 10^6 \ (1.3 \times 10^6)^c$	$(4.39 \pm 0.55) \times 10^5 \ (3.5 \times 10^5)^c$	$(1.12 \pm 0.12) \times 10^4$	$(5.28 \pm 2.27) \times 10^3$
	ΔH			3.79 ± 0.08	3.01 ± 0.04	3.23 ± 0.32	0.79 ± 0.40
	$T\Delta S$			12.32	10.70	8.75	5.86
3	n			0.98 ± 0.01	0.98 ± 0.02		
	K_{app}	a	b	$(8.34 \pm 0.11) \times 10^5 \ (7.9 \times 10^5)^d$	$(4.99 \pm 0.34) \times 10^4 \ (2.9 \times 10^4)^d$	$>10^3$	$>10^3$
	ΔH			4.49 ± 0.07	3.26 ± 0.07		
	$T\Delta S$			12.56	9.66		

[a] Accurate value cannot be obtained under the ITC measurement condition. [b] Due to the insolubility of the peptide, the data cannot be obtained. [c] Apparent binding constant of **1** obtained by the fluorescence titration under the same condition (50 mM HEPES buffer, pH 7.2). [d] Apparent binding constant of **2** obtained by the fluorescence titration under the same condition (50 mM HEPES buffer, pH 7.2).

100 μM in 50 mM HEPES, pH 7.2), the ITC experiment using **2** with peptides was not successful.[18] Alternatively, receptor **3**, which does not self-aggregate under the same condition, was used as a structurally related analogue of **2**. All of the ITC experiments were endothermic ($\Delta H > 0$), and the stoichiometry (values n) was approximately 1. The evaluated binding constants for peptide-c and peptide-d are in good agreement with those obtained by fluorescence titration under the same conditions (Table 3). The binding of **1** to peptide-a is also an endothermic process. However, in this combination, the apparent binding constant cannot be accurately evaluated because of its very strong affinity. Unfortunately, the heat formation is too small and sharply saturated by the addition of 1 equiv of peptide-a even at a low concentration (25 μM). This suggests that the binding affinity of **1** to peptide-a is considerably stronger than that of the other peptides ($K_{app} > 10^7$ M^{-1}). The binding constants of **1** to peptide-e and peptide-f, which cannot be fluorometrically detected, were successfully determined to be $(1.12 \pm 0.12) \times 10^4$ and $(5.28 \pm 2.27) \times 10^3$ M^{-1}, respectively. These are more than 100-fold smaller than the values for peptide-a and peptide-b. On the other hand, the interaction of **3** with peptide-e and peptide-f is too weak to be detected ($K_{app} < 10^3$ M^{-1}). As summarized in Table 3, the order of the binding constant is comparable to that estimated by the fluorescence titration experiments. Therefore, we can conclude that the fluorescence change in the receptors directly reflects the binding to the phosphorylated peptides.

Both the fluorescence and ITC experiments have undoubtedly demonstrated that the receptors can discriminate the sequence of the phosphorylated peptide and more strongly bind to the negatively charged one. Since the present binuclear Zn(II)−Dpa-receptors possess a tetracationic character, it is reasonable to explain that the electrostatic attraction can assist with the coordination interaction between the receptors and the negatively charged peptides, whereas the electrostatic repulsion significantly suppresses the affinity toward the positively charged peptides such as peptide-e and peptide-f. The resulting order of the binding constants for these peptides in our experiments is consistent with this explanation. It is noteworthy that even the structurally simple receptors show such a sequence-dependent recognition toward the phosphorylated peptides as a fundamental binding motif.

Mechanism on Fluorescence Sensing toward Phosphorylated Peptide. The artificial receptors **1** and **2** can selectively
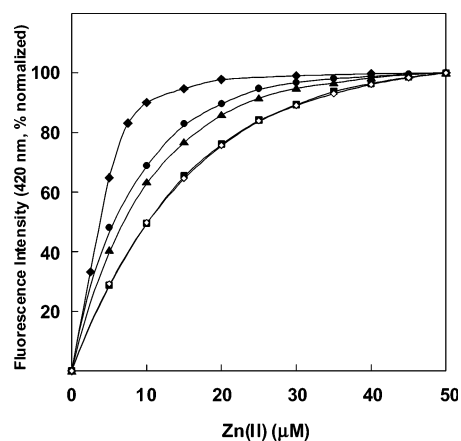

Figure 6. Fluorescence response of the Zn(II)-free ligand of **1** (5 μM, λ_{ex} = 370 nm) to Zn(II) concentration in 50 mM HEPES buffer, pH 7.2: **1** (■) and **1** in the presence of 1 equiv of p-Tyr (▲), 4 equiv of p-Tyr (●), 2 equiv of peptide-a (◆), and 10 equiv of dimethyl phosphate (◇).

sense phosphorylated peptides by the fluorescence change as mentioned above. How does the binding cause the fluorescence intensification in this system?

Under neutral pH conditions, the fluorescence of **1** and **2** due to the anthracene moiety is intensified by the addition of Zn(II) (Figure 6). This fluorescence enhancement is reasonably explained by Zn(II) coordination to the benzylic amine of the Dpa site as previously shown by de Silva et al. using a mono-Dpa derivative (**4**).[19] Such canceling of the photoinduced electron-transfer (PET) process by coordination of a d^{10} metal to an amine (reductive quencher) is a commonly observed mechanism for the fluorescence enhancement.[20]

Figure 6 shows the Zn(II) concentration dependence of the fluorescence intensity of the Zn(II)-free ligand of **1**. Under neutral pH conditions, the fluorescence intensification does not saturate with 2 equiv of Zn(II), but more than 5 equiv of Zn(II) is required for saturation. This suggests that Zn(II) does not completely coordinate to the two Dpa sites of Zn(Dpa)−**1** under the lower receptor concentration (5 μM). Although it is difficult to separately determine the complexation constants of the first and second Zn(II) from the fluorescence change, we can approximately estimate the complexation constant of the free

(18) The complicated and broadened signals were observed in the ^{1}H NMR spectrum of **2** in D$_2$O (0.1 mM), indicating that the present species is not monomeric but aggregates under such a high-concentration condition.

(19) de Silva, S. A.; Zavaleta, A.; Baron, D. E. *Tetrahedron Lett.* **1997**, *38*, 2237.

(20) (a) de Silva, A. P.; Gunaratne, H. Q. N.; Gunnlaugsson, T.; Huxley, A. J. M.; McCoy, C. P.; Rademacher, J. T.; Rice, T. E. *Chem. Rev.* **1997**, *97*, 1515. (b) Burdette, S. C.; Frederickson, C. J.; Bu, W.; Lippard, S. J. *J. Am. Chem. Soc.* **2003**, *125*, 1778. (c) Burdette, S. C.; Walkup, G. K.; Spingler, B.; Tsien, R. Y.; Lippard, S. J. *J. Am. Chem. Soc.* **2001**, *123*, 7831. (d) Hirano, T.; Kikuchi, K.; Urano, Y.; Nagano, T. *J. Am. Chem. Soc.* **2002**, *124*, 6555.

Scheme 1. Schematic Representation of the Sensing Mechanism of the Receptors toward the Phosphorylated Peptide
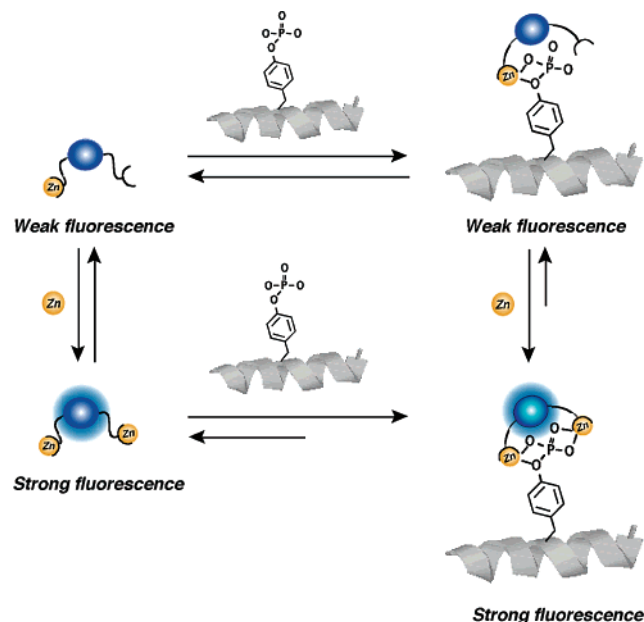
ligand **1** corresponding to the first and second Zn(II) binding to be $>1 \times 10^6$ and $\sim 3 \times 10^5$ M^{-1}, respectively.[21] The value for the second Zn(II) complexation is much smaller than that of the mono-Dpa ligand of **4** (6.6×10^6 M^{-1}) with Zn(II). The lower affinity of the second Zn(II) to Dpa is probably due to the electrostatic repulsion between the positively charged first Zn(Dpa) site and the incoming second Zn(II) cation.[20c] Importantly, when Zn(II) was added to the free ligand of **1** in the presence of p-Tyr, the fluorescence change was more sharply saturated depending on the amount of p-Tyr (1 or 4 equiv) relative to that in the absence of p-Tyr (Figure 6). This indicates that coordination of the second Zn(II) to the free Dpa site is facilitated by p-Tyr. The same magnitude of enhancement was also observed with phosphate, MeP, and the phosphorylated peptide-d (data not shown). Interestingly, in the presence of the peptide-a, which can bind to **1** with the highest affinity ($K_{app} = 8.9 \times 10^6$ M^{-1} determined by fluorescence titration) among the phosphorylated peptides, the fluorescence change was saturated with almost 2 equiv of Zn(II), whereas the excess amount of diMeP (10 equiv) which cannot bind to receptor **1**, does not cause any facilitation effect on the Zn(II) coordination (Figure 6). Almost the same tendency was observed for receptor **2** (data not shown).

These results strongly suggest that the fluorescence intensification of the receptors (**1** or **2**) induced by the phosphate derivatives is mainly attributable to the phosphate-assisted coordination of the second Zn(II). A schematic illustration of the sensing mechanism of the receptors toward the phosphorylated peptide is depicted in Scheme 1. In the absence of a

phosphorylated peptide, the second Dpa site of the receptor is partially free so that PET quenching by the benzylic amine of Dpa lessens the fluorescence of anthracenes. In the presence of a phosphorylated peptide, coordination of the second Zn(II) to the free Dpa site is facilitated, and as a result, PET quenching is suppressed and the fluorescence intensity recovers.

As shown in Figure 4b, we observed that the magnitude of the fluorescence enhancement (F_{max}/F_o) becomes greater with an increase of the negative net charge of the peptides. One reason for this phenomenon is that the net fluorescence intensity becomes nonlinearly weak with decreasing the receptor concentration in the micromolar concentration range due to the small association constant for the second Zn(II) binding ($\sim 3 \times 10^5$ M^{-1}). Thus, at the lower concentration of the receptor (1 μM in the titration with peptide-a, -b, -c), a fraction of the weak fluorescent mononuclear Zn(II)$-$**1** increases compared to that for the higher concentration (5$-$10 μM in the titration with peptide-d, -e, -f). The addition of the phosphorylated peptide changes the equilibrium where a fraction of the binuclear Zn-(II)$-$**1** binding to the phosphorylated peptide is predominant under the saturation binding condition. Therefore, the relative change ratio in the fluorescence intensity is greater for the low-concentration experiment than that at the high concentration. In fact, F_{max}/F_o obtained from the titration experiments with peptide-c using 10 μM of **1** is almost half compared to that using 1 μM **1** (data not shown). However, in the titration with peptide-a, -b, and -c, F_{max}/F_o becomes greater with an increase of negative net charge of the peptides even though the titration is conducted with the identical concentration of **1** (1 μM). This phenomenon is more clearly observed in the case of **2** (see Supporting Information). These results suggest that the phosphate-assisted coordination of the second Zn(II) is influenced by the negative net charge of the peptide; that is, a highly negative phosphorylated peptide such as peptide-a may electrostatically facilitate the coordination of the second Zn(II) to the Dpa to result in the greater enhancement of the fluorescence intensity.[22]

Fluorescent Monitoring of Phosphatase-Catalyzed Dephosphorylation. On the basis of these fundamental findings, we finally investigated the utility of these artificial receptors for phosphatase activity assay. In a proof-of-principle experiment, protein tyrosine phosphatase 1B (PTP1B) as an enzyme and the corresponding phosphorylated peptide, DADE-pY-LIPNNG (a fragment (988$-$998) of EGFR), as a substrate were employed. According to the above-mentioned binding data, the receptors show a higher affinity to the anionic substrate peptide than to the product phosphate, so that the fluorescence intensity is reasonably different under suitable conditions. As expected, the emission intensity of the receptors in the presence of 1 equiv of the substrate peptide (F_{pep}) is stronger relative to that in the presence of 1 equiv of phosphate anion (F_{phos}) under the assay condition; i.e., $F_{pep}/F_{phos} = 1.7$ for **1** (420 nm) and 2.7 for **2** (434 nm), respectively (see Supporting Information). Using the fluorescence plate reader technique, we can monitor the time trace of the PTP1B-catalyzed dephosphorylation reaction as shown in Figure 7. The fluorescence decreases with the addition of PTP1B in its intensity according to the approximate first-

(21) The fluorescent titration experiment of **1** (1 μM) with Zn(NO$_3$)$_2$ showed that the titration curve for the fluorescence change ($\lambda_{em} = 420$ nm) fitted well to the theoretical curve assuming a 1:1 complex and afforded a Zn(II) complexation constant of $(3.0-3.2) \times 10^5$ M^{-1}. Since the complexation constant corresponding to the first Zn(II) of **1** should be almost the same value with that of the mono-Dpa ligand of **4** (6.6×10^6 M^{-1}), the first Zn(II) complexation has almost completed within 2 equiv of Zn(II) under the titration condition. Thus, we concluded the obtained value ($\sim 3 \times 10^5$ M^{-1}) should correspond to the second Zn(II) binding to **1**. The second Zn(II) complexation constant of **2** was also obtained as $\sim 7 \times 10^4$ M^{-1} from a similar fluorescent titration experiment.

(22) Since the Zn(II) centers of the receptors have one accessible site even after phosphate binding (see Figure 3), the neighboring carboxylate groups of the anionic peptides may be involved in the coordination to the Zn(II) centers so as to enhance the second Zn(II) complexation more efficiently. This may be another plausible mechanism for the strong affinity and large fluorescence change toward the anionic peptides.
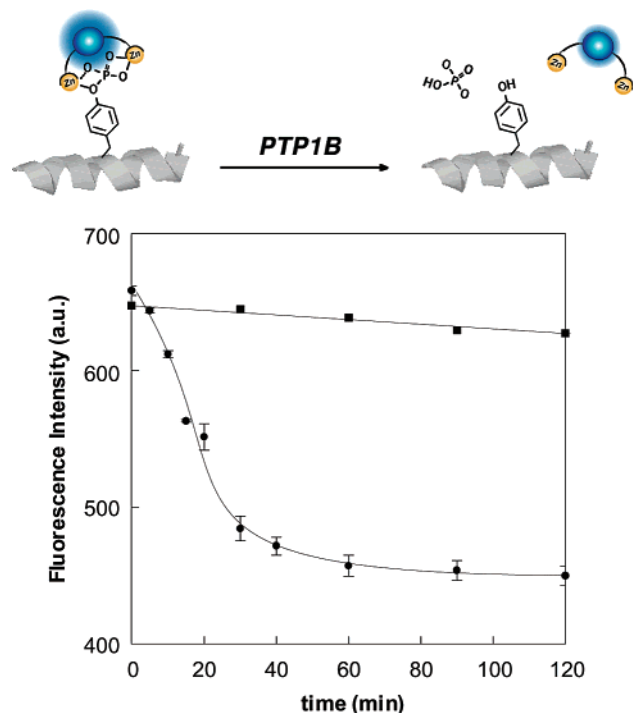
Figure 7. (Top) Schematic illustration of the fluorescence detection of the PTP1B catalyzed dephosphorylation. (Bottom) Time trace of the PTP1B-catalyzed dephosphorylation monitored by the emission at 420 nm of **1** (excited at 370 nm) with (●) or without (■) PTP1B using the fluorescence plate reader.

order kinetics for both receptors **1** and **2** (see Supporting Information) as a probe. In contrast, the fluorescence did not change without PTP1B. The dephosphorylation process of the peptides can be qualitatively monitored by MALDI-TOF mass spectroscopy as an alternative method. However, a quantitative analysis is sometimes difficult because the ionization tendency of peptides is greatly dependent on the phosphorylation. In fact, the mixture of the phosphorylated EGFR fragment peptide with the nonphosphorylated one (10:1 ratio) gave a varied peak intensity between 2:1 and 1:4 by MALDI-TOF mass spectrometry depending on the measurement conditions (data not shown). It is clear that the present receptors are useful for the fluorescent phosphatase activity assay in the convenient and quantitative manner.

Conclusion

In this study, we presented the molecular recognition and fluorescence sensing features of the anthracene binuclear Zn-(II)−Dpa complex toward the phosphorylated peptides. Our experimental results clearly indicated that receptors **1** and **2** can effectively bind to a phosphate group on a peptide under neutral aqueous conditions by the cooperative use of the metal−ligand interaction of the two Zn(II)−Dpa sites. It is also clear that receptors **1** and **2** not only discriminate the phosphorylated peptides from the nonphosphorylated one but also show the sequence-dependent affinity toward the series of phosphorylated peptides depending on the electrostatic interaction between them. Indeed, the highly negatively charged peptide-a is bound to the cationic receptors with a nearly 10^7 M^{-1} binding affinity. To our knowledge, this value is one of the largest binding constants of a synthetic receptor to a monophosphate species in water reported so far. A unique fluorescence sensing mechanism

involved the efficient canceling of PET quenching through the phosphate anion induced Zn(II) complexation. Furthermore, we successfully demonstrated that the present receptors can be applied to fluorometric monitoring of the enzyme-catalyzed dephosphorylation. This technique using our artificial receptors should be readily extended to a screening assay for certain kinds of phosphatase inhibitors, including the PTP1B inhibitor that has been a promising therapeutic agent for type II diabetes and obesity.[23]

Thus, the receptors presented herein are a novel type of chemosensor that can directly bind and sense phosphorylated peptide surface.[24] Although the binding selectivity of the receptors between the phosphorylated peptides and biological pyrophosphate derivatives (ATP, ADP) is not satisfactory, elaborated structural modification could provide artificial chemoreceptors with a high recognition selectivity toward a phosphorylated protein surface. Furthermore, such artificial receptors may serve a potential regulator of protein surface interactions as well as a fluorescent chemosensor, since the phosphate group attached on the protein surface acts as a pinpoint residue critical to protein−protein interactions and significantly contributes to the stability of the complex. We are now underway along this line.

Experimental Section

Syntheses of the Zn^{II}−dpa Type of Receptors. The Zn(II)-free ligands of the complexes (**1**−**5**) were synthesized from the corresponding halomethyl compounds by the reaction with 2,2′-dipicolylamine and potassium carbonate in anhydrous dimethylformamide (DMF) at ambient temperature as described previously.[5] The Zn(II) complexes (**1**−**5**) were obtained after the treatment of the corresponding ligand with a solution of zinc(II) nitrate in appropriate solvent at room temperature. Typical synthetic procedures are as follows:

1,8-Bis[(2,2′-dipicolylamino)methyl]anthracene Zinc Complex (1). To a solution of 2,2′-dipicolylamine (1.23 g, 6.16 mmol), K$_2$CO$_3$ (1.55 g, 11.2 mmol), and KI (464 mg, 2.80 mmol) in anhydrous DMF (20 mL) was added portionwise 1,8-bis(chloromethyl)anthracene[5] (770 mg, 2.80 mmol), and the reaction mixture was stirred for 8 h at room temperature. After dilution with tetrahydrofuran (THF), the mixture was acidified with 2 N HCl and then washed with AcOEt. The aqueous layer was alkalized with 4 N NaOH, and extracted with AcOEt (×2). The combined organic layers were washed with water and brine followed by drying over MgSO$_4$. After removal of the solvent in vacuo, the obtained solid was filtered and washed with AcOEt to give 1,8-bis[(2,2′-dipicolylamino)methyl]anthracene (1.27 g, 76%) as a pale yellow powder. ^{1}H NMR (600 MHz, CDCl$_3$): δ 5.23 (4H, s), 7.45 (t, $J = 7.5$ Hz, 2H), 7.58 (2H, d, $J = 6.6$ Hz), 8.03 (2H, d, $J = 8.5$ Hz),

(23) (a) Szczepankiewicz, B. G.; Liu, G.; Hajduk, P. J.; Abad-Zapatero, C.; Pei, Z.; Xin, Z.; Lubben, T. H.; Trevillyan, J. M.; Stashko, M. A.; Ballaron, S. J.; Liang, H.; Huang, F.; Hutchins, C. W.; Fesik, S. W.; Jirousek, M. R. *J. Am. Chem. Soc.* **2003**, *125*, 4087. (b) Johnson, T. O.; Ermolieff, J.; Jirousek, M. R. *Nat. Rev. Drug Discovery* **2002**, *1*, 696.

(24) Protein surface recognition: (a) Veselovsky, A. V.; Ivanov, Y. D.; Ivanov, A. S.; Archakov, A. I.; Lewi, P.; Janssen, P. *J. Mol. Recognit.* **2002**, *15*, 405. (b) Peczuh, M. W.; Hamilton, A. D. *Chem. Rev.* **2000**, *100*, 2479. (c) Ojida, A.; Inoue, M.; Mito-oka, Y.; Hamachi, I. *J. Am. Chem. Soc.* **2003**, *125*, 10184. (d) B-Sikder, K.; Kodadek, T. *J. Am. Chem. Soc.* **2003**, *125*, 9550. (e) Kutzki, O.; Park, H. S.; Ernst, J. T.; Orner, B. P.; Yin, H.; Hamilton, A. D. *J. Am. Chem. Soc.* **2002**, *124*, 11838. (f) Fazal, M. A.; Roy, B. C.; Sun, S.; Mallik, S.; Rodgers, K. R. *J. Am. Chem. Soc.* **2001**, *123*, 6283. (g) Blaskovich, M. A.; Lin, Q.; Delarue, F. L.; Sun, J.; Park, H. S.; Coppola, D.; Hamilton, A. D.; Sebti, S. M. *Nat. Biotechnol.* **2000**, *18*, 1065. (h) Takashima, H.; Shinkai, S.; Hamachi, I. *Chem. Commun.* **1999**, 2345. (i) Hamachi, I.; Fujita, A.; Kunitake, T. *J. Am Chem. Soc.* **1997**, *119*, 9096. (j) Jain, R. K.; Hamilton, A. D. *Org. Lett.* **2000**, *2*, 1721. (k) Tabet, M.; Labroo, V.; Sheppard, P.; Sasaki, T. *J. Am. Chem. Soc.* **1993**, *115*, 3866.

8.51 (1H, s), 9.00 (1H, s). FAB-MS $C_{40}H_{36}Cl_6$: m/e 601 [M]$^+$. Anal. Calcd for $C_{40}H_{36}N_6$: C, 79.97; H, 6.04; N, 13.99. Found: C, 79.48; H, 6.08; N, 13.63.

To a solution of 1,8-bis[(2,2′-dipicolylamino)methyl]anthracene (400 mg, 0.67 mmol) in CH$_3$CN−THF (5:1, 24 mL) was added dropwise 112 mM Zn(NO$_3$)$_2$ in MeOH (11.96 mL, 1.34 mmol)). After stirring for 30 min at room temperature, the precipitate was filtered and washed with CH$_3$CN to give **1** (540 mg, 79%) as a colorless powder: FAB-MS $C_{40}H_{36}N_6$·2Zn·3NO$_3$: m/e 916 [M − NO$_3$]$^+$. UV (in H$_2$O) λ_{max} = 255, 352, 371, 390 nm. Anal. Calcd for $C_{40}H_{36}N_6$·2Zn·4NO$_3$: C, 49.05; H, 3.70; N, 14.30. Found: C, 49.05; H, 3.74; N, 14.28.

9,10-Bis[(2,2′-dipicolylamino)methyl]anthracene Zinc Complex (2). ^{1}H NMR (600 MHz, DMSO-d_6 + D$_2$O (DMSO = dimethyl sulfoxide)): δ 3.92 (br s, 4H), 4.02 (br s, 4H), 4.74 (s, 2H), 4.88 (s, 2H), 7.23−7.25 (br m, 4H), 7.38 (br d, 2H), 7.54 (s, 2H), 7.66 (br d, 2H), 7.70 (br d, 2H), 7.92 (br d, 2H), 8.03 (br s, 4H), 8.42 (s, 2H), 8.61 (br d, 2H), 8.68 (br s, 2H). FAB-MS $C_{40}H_{36}N_6$·2Zn·3NO$_3$: m/e 916 [M − NO$_3$]$^+$. UV (in H$_2$O) λ_{max} = 259, 364, 381, 403 nm. Anal. Calcd for $C_{40}H_{36}N_6$·2Zn·4NO$_3$·2H$_2$O: C, 47.31; H, 3.97; N, 13.79. Found: C, 47.20; H, 3.93; N, 13.74.

1,4-Bis[(2,2′-dipicolylamino)methyl]benzene Zinc Complex (3). FAB-MS $C_{32}H_{32}N_6$·2Zn·3NO$_3$: m/e 816 [M − NO$_3$]$^+$. Anal. Calcd for $C_{32}H_{32}N_6$·2Zn·4NO$_3$: C, 43.70; H, 3.67; N, 15.93. Found: C, 43.70; H, 3.67; N, 15.93.

9-[(2,2′-Dipicolylamino)methyl]anthracene Zinc Complex (4). FAB-MS $C_{27}H_{23}N_3$·Zn·NO$_3$: m/e 515 [M − NO$_3$]$^+$. Anal. Calcd for $C_{27}H_{23}N_3$·Zn·2NO$_3$·3H$_2$O: C, 51.24; H, 4.62; N, 11.06. Found: C, 51.40; H, 4.52; N, 11.07.

(2,2′-Dipicolylamino)methylbenzene Zinc Complex (5). FAB-MS $C_{19}H_{19}N_3$·Zn·NO$_3$: m/e 415 [M − NO$_3$]$^+$. Anal. Calcd for $C_{19}H_{19}N_3$·Zn·2NO$_3$: C, 47.66; H, 4.00; N, 14.63. Found: C, 47.73; H, 4.00; N, 14.61.

Solid-Phase Peptide Synthesis. All peptides were synthesized by an automated peptide synthesizer (ABI 433A, Applied Biosystems) using the standard Fmoc-based FastMoc coupling chemistry (0.1 mmol scale) with Fmoc-Amide Resin (Applied Biosystems). Fmoc-Ser[PO-(OBzl)OH]-OH and Fmoc-Tyr[PO(OBzl)OH]-OH (Watanabe Chemical Industries, Ltd.) were used as the phosphorylated amino acid unit for the peptide coupling. After the automated solid-phase peptide synthesis (SPPS), the peptide was acetyl-capped with 20% Ac$_2$O in CH$_2$Cl$_2$ over 2 h followed by cleaving from resin by treatment with TFA−*m*-cresol−thioanisole (86:2:12) over 1 h. Crude peptide was precipitated in *tert*-butyl methyl ether, and purified by reverse-phase HPLC (column; YMC-pack ODS-A, 250 × 10 mm). The purification conditions were as follows: mobile phase, CH$_3$CN (containing 0.1% TFA)/H$_2$O (containing 0.1% TFA) = 5/95 → 40/60 (linear gradient over 60 min); flow rate, 3 mL/min; detection, UV (220 nm). Molecular weight of the peptide was confirmed by mass spectrometer (MALDI-TOF): peptide-a, calcd (found) for $C_{55}H_{75}N_{10}O_{26}P$ [M]$^+$, m/e 1345.4 (1346.0); peptide-b, calcd (found) for $C_{56}H_{73}N_{10}O_{22}P$ [M + Na]$^+$, m/e 1291.5 (1292.1); peptide-c, calcd (found) for $C_{52}H_{77}N_{10}O_{18}P$ [M + Na]$^+$, m/e 1183.5 (1183.7); peptide-d, calcd (found) for $C_{39}H_{63}N_{10}O_{18}P$ [M]$^+$, m/e 990.4 (991.1); peptide-e, calcd (found) for $C_{43}H_{73}N_{16}O_{14}P$ [M + H]$^+$, 1069.5 (1069.8); peptide-f, calcd (found) for $C_{55}H_{91}N_{22}O_{14}P$ [M + H]$^+$, m/e 1315.7 (1316.1); peptide-g, calcd (found) for $C_{55}H_{74}N_{10}O_{23}$ [M + Na]$^+$, 1265.4 (1266.2).

NMR Study. ^{1}H NMR study of **1** with p-Tyr (Figure 2) was measured on a Brucker DRX-600 (600 MHz) at 25 ± 1 °C. Samples were prepared using a concentration of 0.1 mM **1** in D$_2$O in the absence or presence of 0.1 mM p-Tyr. pD was adjusted to be 7.1 ± 0.1 by addition of a small amount of NaOD. TSP was used as an internal standard, and the observed peaks were individually assigned by the COSY experiments. ^{31}P NMR spectra were recorded on a Brucker DRX-600 (243 MHz) at 25 ± 1 °C. Samples were prepared using a

concentration of 0.2 mM phosphate species in 50 mM HEPES (pH 7.2) buffer/D$_2$O (90:10) in the absence and presence (1 equiv) of **1**. A 0.1 mM amount of H$_3$PO$_4$ in H$_2$O was used as an external standard.

X-ray Crystallography. X-ray diffraction data were collected on a Rigaku R-AXIS RAPID diffractometer with a 2D area detector using graphite-monochromatized Cu Kα radiation (λ = 1.5418 Å) at ca. 120 K. Lattice parameters were obtained by least-squares analysis from reflections for three oscillation images. Direct methods (SIR92) were used for the structure solution. All calculations were performed using on the TEXSAN[25] crystallographic software package. All non-hydrogen atoms except one of the two nitrates are found by Fourier syntheses due to server disorder. Trials to find and refine the disordered nitrate were found to be without success. The structure was refined by full matrix least-squares procedure using observed reflections ($>2.0\sigma(I)$) based on F^2, and all non-hydrogen atoms except the disordered nitrate were refined with anisotropic displacement parameters and hydrogen atoms were placed in idealized positions with isotropic displacement parameters relative to the connected non-hydrogen atoms and not refined. Crystallographic parameters are summarized in the Supporting Information.

Fluorescence Titration. Fluorescent spectra were recorded on a Perkin-Elmer LS55 spectrometer. The titration experiments with NaH$_2$PO$_4$, phenyl phosphate (PhP), *O*-phospho-l-tyrosine (p-Tyr), methyl phosphate (MeP), and dimethyl phosphate (diMeP) (Figure 1, Table 1) were conducted with a solution of **1** (5 μM) or **2** (10 μM) in 10 mM HEPES buffer (pH 7.2), and the titration experiments with the AXP species (ATP, ADP, AMP, cAMP) were conducted with a solution of **1** (1−5 μM) or **2** (5−10 μM) in 50 mM NaCl, 50 mM HEPES buffer (pH 7.2). In the titration experiment of **1** with the phosphorylated peptides (Figure 4, Table 2), 1 μM (with peptide-a, -b, -c, and -g), 5 μM (with peptide-d), and 10 μM (with peptide-e and -f) solutions of **1** in 50 mM NaCl, 50 mM HEPES buffer (pH 7.2) were employed. In the case of **2**, 1 μM (with peptide-a, -b, and -g), 5 μM (with peptide-c and -d), and 10 μM (with peptide-e and -f) solution of **2** in 10 mM NaCl, 50 mM HEPES buffer (pH 7.2) were employed. All titration experiments were carried out with 3 mL of the receptor solution in a quartz cell (excitation wavelength: λ_{ex}(**1**) = 370 nm, λ_{ex}(**2**) = 380 nm) at 20 ± 1 °C, and the fluorescence emission change was monitored upon the addition of the freshly prepared aqueous stock solution of the phosphate species or peptide with a microsyringe. Fluorescent titration curves (λ_{em}(**1**) = 420 nm, λ_{em}(**2**) = 434 nm) were analyzed with the nonlinear least-squares curve-fitting method to evaluate the apparent binding constant (K_{app}, M^{-1}).

ITC Experiment. ITC titration was performed on an Isothermal Titration Calorimeter from MicroCal Inc. All measurements were conducted at 298 K. In general, a solution of the peptide (1−2 mM) in 50 mM HEPES buffer (pH 7.2) was injected stepwise (10 μL × 24 times) to a solution of **1** or **3** (25−100 μM) dissolved in the same solvent system. The measured heat flow was recorded as function of time and converted into enthalpies (ΔH) by integration of the appropriate reaction peaks. Dilution effects were corrected by subtracting the results of a blank experiment with a solution of 50 mM HEPES solution (pH 7.2) in place of the peptide solution under identical experimental conditions. The binding parameters (K_{app}, ΔH, ΔS, n) were evaluated by applying one site model using the software Origin (MicroCal Inc.).

Fluorescent PTP1B Assay. The phosphorylated peptide (EGFR 988−998) and PTP1B were purchased from CALBIOCHEM. Fluorescence spectra were measured by a Perkin-Elmer LS55 spectrometer equipped with a Plate Reader accessory.

The preincubated (30 °C) solution of the phosphorylated peptide (EGFR 988−998) (160 μL) in assay buffer (50 mM HEPES, 1 mM

(25) *TEXSAN*, X-ray structure analysis package; Molecular Structure Corp.: The Woodlands, TX, 1985.

DTT, 1 mM EDTA, 0.1% NP-40, pH 7.2) was mixed with 40 μL of PTP1B (1200 U) to initiate the enzymatic reaction (final concentration of the substrate peptide is 150 μM). During the reaction, 20 μL of the incubated solution was sampled and mixed with 20 μL of CH_3CN at each time (0, 5, 10, 15, 20, 30, 40, 60, 90, and 120 min) to terminate the reaction. The terminated solutions (10 μL) were mixed with 140 μL of the receptor solution (5 μM of **1** or **2**, 30 μM of zinc(II) nitrate, 50 mM HEPES, pH 7.2) on a 96-well microplate, and the fluorescence intensities of each well (λ_{em} = 420 nm for **1** (λ_{ex} = 370 nm), λ_{em} = 434 nm for **2** (λ_{ex} = 380 nm)) were automatically measured with the plate reader.